

Supplemental Material for: Inhibiting mitochondrial respiration prevents cancer in a mouse model of Li-Fraumeni syndrome

Authors: Ping-yuan Wang^{1*}, Jie Li^{1*}, Farzana L. Walcott^{2,3}, Ju-Gyeong Kang¹, Matthew F. Starost⁴, S. Lalith Talagala⁵, Jie Zhuang¹, Ji-Hoon Park¹, Rebecca D. Huffstutler¹, Christina M. Bryla⁶, Phuong L. Mai², Michael Pollak⁷, Christina M. Annunziata⁶, Sharon A. Savage², Antonio Tito Fojo⁸, Paul M. Hwang¹

Affiliations:

¹Center for Molecular Medicine, National Heart, Lung, and Blood Institute, NIH, Bethesda, Maryland, USA

²Division of Cancer Epidemiology and Genetics, National Cancer Institute, Rockville, Maryland, USA

³Department of Internal Medicine, George Washington University, Washington, DC, USA

⁴Division of Veterinary Resources, NIH, Bethesda, Maryland, USA

⁵NIH MRI Research Facility, National Institute of Neurological Disorders and Stroke, NIH, Bethesda, Maryland, USA

⁶Center for Cancer Research, National Cancer Institute, Bethesda, Maryland, USA

⁷Departments of Oncology and Medicine, McGill University, Montreal, Canada

⁸Division of Hematology and Oncology, Columbia University Medical Center, New York, USA

*These authors contributed equally to this work.

Corresponding author e-mail: hwangp@mail.nih.gov

Supplemental Methods

Human studies

All subjects were enrolled after informed consent as approved by the NCI and NHLBI Institutional Review Boards (ClinicalTrials.gov identifiers NCT01981525 and NCT00406445, respectively). Participation in the studies required a diagnosis of Li-Fraumeni syndrome by *TP53* genetic testing. Participants were also required to be in good health based on medical record review, history and physical examination, and laboratory tests. None of the LFS subjects had active cancer diagnosis or were on cancer treatment at the time of enrollment. After pretreatment testing (week 0), metformin was initiated at 500 mg p.o. daily with dose escalation by 500 mg increments every 2 wk until 2000 mg or the maximum tolerated dose was achieved. Of the participants in this study, only one patient did not achieve the 2000 mg daily dose due to minor side effects but tolerated 1500 mg daily. Following a total of 8 wk at the maximum tolerated dose of metformin (week 14), subjects were tested again after a 6 wk medication washout period (week 20). A comprehensive analysis of the safety and tolerability of metformin in the "Pilot Study of Metformin in Patients with a Diagnosis of Li-Fraumeni Syndrome" (NCT01981525) will be reported separately (1).

Mouse studies

All mice were maintained and handled in accordance with the NHLBI Animal Care and Use Committee. Experimental mouse models were obtained from the following sources: wild-type (Jackson Laboratories); heterozygous *p53*^{172R/H} (NCI Frederick Mouse Repository, Frederick, MD) (2); and heterozygous *Polg*^{+/*mut*} (T. Finkel, NIH, Bethesda, MD, originally created by T. A.

Prolla and colleagues, University of Wisconsin, Madison, WI) (3). All mice were of the C57BL6 strain or backcrossed at least 5 generations into the C57BL6 background. Unless otherwise noted, all mice used for experiments were healthy without overt evidence of cancer and male due to the difficulty in obtaining female homozygous $p53^{172H/H}$ mice. For cancer-free survival studies, endpoint guidelines approved by the NHLBI Animal Care and Use Committee were followed. Specifically, animals were euthanized if any external mass exceeded 2 cm in its largest dimension or when the mouse met moribund criteria on assessment by study investigators and veterinary technicians. All necropsies and histopathologic diagnosis were made by qualified veterinary pathologists of the Division of Veterinary Resources, NIH. Blood lactate level in the second drop of blood obtained by tail nick was measured using the Lactate Plus test strip and meter (Nova Biomedical, Waltham, MA).

Metformin treatment of mice

Mice fed metformin dissolved at 1 mg/ml drinking water have been shown to consume ~250 mg/kg body weight per day to achieve a plasma concentration of 0.45 μ g/ml, which is a concentration within range of that reported in humans on metformin treatment (4). Based on the average volume of water consumed by $p53^{R172H/H}$ mice, we confirmed that metformin dissolved at 0.2 mg/ml and 1.25 mg/ml of metformin (Sigma cat. no. D150959) was sufficient to deliver ~50 mg/kg/d and ~250 mg/kg/d, respectively. For the survival study, mice were randomly divided and either maintained on control drinking water or initiated on metformin treatment after weaning (age ~4 wk old).

Cell culture

Wild-type (*SCO2*^{+/+}) human colon cancer (HCT116) and immortalized human T lymphocyte (Jurkat) cell lines were obtained from American Type Culture Collection and cultured in McCoy's 5A (supplemented with 10% FBS) or RPMI 1640 (supplemented with 10% FBS and 50 μ M 2-mercaptoethanol) medium, respectively. The generation of non-respiring isogenic *SCO2*^{-/-} HCT116 cell line has been reported previously (5). Primary human myoblasts were obtained and cultured as previously described (6).

cDNA constructs and lentivirus transduction

The R175H mutation was introduced into human p53 cDNA using Quickchange II site-directed mutagenesis kit (Agilent technologies). Mutation was confirmed by sequencing, and the p53 cDNA was subcloned into pLEX-MCS plasmid (OpenBiosystems) for lentivirus preparation.

The lentiviruses were produced using Mission lentiviral packaging mix (Sigma-Aldrich). Cells were incubated with virus for 24 h followed by one week of 2 μ g/ml puromycin selection prior to experiment.

Antibodies

Antibodies used in this study were obtained from the following sources: actin mouse mAb (A3853), actinin mouse mAb (A7811), LC3 rabbit polyclonal antibody (pAb, L8918) (Sigma, St. Louis, MO); GSK3 α/β rabbit pAb (#9331), phospho-GSK3 α/β (Ser9/21) rabbit pAb (#9336), cyclin D1 mouse mAb (DCS6), cyclin E1 mouse mAb (#4129), phospho-AMPK α (Thr172) rabbit mAb (#2535), PTEN rabbit pAb (#9552), AKT rabbit pAb (#9272), phospho-AKT (Ser473) rabbit pAb (#9271), cleaved-caspase 3 rabbit mAb (#9664) (Cell Signaling, Danvers,

MA); hexokinase 2 goat pAb (sc-6521), p53 mouse mAb (DO-1, sc-126), phospho- GSK3 α/β (Tyr-279/216) rabbit pAb (sc-135653), cyclin D1 rabbit pAb (sc-753), ND4 rabbit pAb (sc-20499), NRF2 rabbit pAb (sc-722) (Santa Cruz Biotech. Inc., Santa Cruz, CA); NQO1 rabbit pAb (ab34173), Lamin B1 rabbit pAb (ab16048), NRF2 rabbit pAb (ab62352), oxidative phosphorylation complex mouse mAb mix (ab110413) (Abcam, Cambridge, MA); GLUT4 rabbit pAb (3945-200) (Biovision, Milpitas, CA); and VDAC rabbit pAb (600-401-882) (Rockland, Limerick, PA).

Western blot analysis

Protein samples were solubilized in cold RIPA buffer with protease and phosphatase inhibitors (Roche Diagnostic Corp.) and subjected to standard Western blotting using SDS/PAGE protein resolution, Immobilon-P membrane protein transfer (Millipore), and ECL development (GE Healthcare).

Cell preparation and Seahorse XF metabolic assay

Human peripheral blood mononuclear cells (PBMCs) were isolated by density centrifugation using citrate-containing Vacutainer CPT tubes (Becton Dickinson). Cell suspensions from mouse thymus were prepared by gently disrupting the tissue on a nylon mesh (100 μm , Millipore) using a flat edged forcep, triturating with a 1 ml pipet tip, filtering through a nylon cell strainer (40 μm , BD Falcon Labware), and washing the cells in cold PBS. The isolated cells (1×10^6) were resuspended in XF assay DMEM medium (Seahorse Bioscience) supplemented with 2 mM Glutamax, 1 mM sodium pyruvate and 25 mM glucose and plated in each well of a XF-24 plate coated with Cell-Tak. After a low speed spin to facilitate cell attachment, the cells

were incubated in a non-CO₂ incubator at 37 °C for ~1 h, and then the oxygen consumption rate (OCR) and extracellular acidification rate (ECAR) were measured as previously described (7). To normalize the results of human samples measured on different days, identical aliquots of frozen Jurkat human T lymphocytes were plated and concurrently assayed with the human PBMCs.

Cell proliferation assay

For measuring the sensitivity of cell growth to metformin, *SCO2*^{+/+} or *SCO2*^{-/-} HCT116 cells were plated at a density of 700 or 2,800 cells per well of a 6-well plate, respectively, and cultured in the indicated concentration of metformin for 10 d. The colonies were then visualized by crystal violet staining and cell number quantified by using an automated cell counter (Invitrogen).

ROS measurements

Dissociated cells (3×10^5) were incubated in 0.5 ml of complete medium containing 5 μM H₂DCFDA (Molecular Probes) in the dark at 37 °C for 15 min, washed twice with PBS, and resuspended in 0.5 ml PBS. H₂O₂-sensitive DCF fluorescence was quantified by flow cytometry (FACS).

Tissue subcellular fractionation

Nuclear fractions were prepared from fresh tissues by using a nuclear extraction kit (Pierce NE-PER), and mitochondria were isolated by using standard techniques as previously described (8).

Blue-native gel and in-gel mitochondrial complex I assay

The mitochondrial complexes were resolved using a Invitrogen NativePAGE 4-16% Bis-Tris gel according to the manufacturer's protocol. In-gel complex I activity was visualized by incubating the gel in 50 ml of buffer containing 50 mM potassium phosphate- pH 7.0, 10 mg Nitro Blue Tetrazolium (NBT), and 5 mg NADH at room temperature for different periods of time. The complex I reaction was stopped by incubating in 50% methanol and 10% acetic acid.

Noninvasive skeletal muscle phosphorus-31 magnetic resonance spectroscopy

Phosphorus-31 magnetic resonance spectroscopy (^{31}P -MRS) of skeletal muscle was performed to measure the depletion of phosphocreatine in the tibialis anterior muscle with foot exercise and to measure its recovery kinetics as a marker of oxidative phosphorylation capacity as previously described (6). Briefly, submaximal exercise was performed by dorsiflexing the foot (~40 times over 2 min) against a custom-built pedal that was attached via a pulley system to 30% of the maximum lifted weight by the subject. ^{31}P spectra were obtained at rest, during exercise and recovery and then analyzed using SAGE (GE Healthcare) and IDL (Exelis Visual Information Solutions) software.

Supplemental Table 1. Effect of mitochondrial disruption on tumor spectrum in the $p53^{172H/H}$ genetic background

Cancer Type	$p53^{172H/H}$				
	Mouse genotype			Metformin treatment	
	Control (n = 42)	$Polg^{+/mut}$ (n = 21)	$Polg^{mut/mut}$ (n = 30)	0.2 mg/ml (n = 22)	1.25 mg/ml (n = 21)
Lymphoma	33 (79%)	14 (67%)	6 (20%)***	18 (82%)	18 (86%)
Rhabdomyosarcoma	7 (17%)	2 (10%)	2 (7%)	3 (14%)	3 (14%)
Hemangiosarcoma	7 (17%)	4 (19%)	5 (17%)	6 (27%)	4 (19%)
Histiocytic sarcoma	3 (7%)	5 (24%)	8 (27%)*	1 (5%)	2 (10%)
Other sarcomas	3 (7%)	0 (0%)	0 (0%)	2 (9%)	0 (0%)
Carcinoma	2 (5%)	0 (0%)	0 (0%)	0 (0%)	0 (0%)
Teratoma	2 (5%)	0 (0%)	0 (0%)	0 (0%)	0 (0%)
CNS tumor	0 (0%)	1 (5%)	1 (3%)	1 (5%)	0 (0%)
Mice with no cancer diagnosis	0 (0%)	0 (0%)	8 (27%)**	1 (5%)	0 (0%)
Thymic lymphoma	31 (74%)	11 (52%)	1 (3%)***	17 (77%)	16 (76%)

Cancer types were diagnosed by necropsy and histopathology by a qualified veterinary pathologist. Control refers to the $p53^{172H/H}$ genetic background, and number of mice in each group is indicated by (n). To demonstrate the involvement of the thymus in $p53^{172H/H}$ mouse tumorigenesis, lymphomas involving the thymus were further sub-classified as thymic lymphomas. Note the lower incidence of thymic lymphoma associated with the $Polg^{mut/mut}$ genotype known to have involution of the thymus. For metformin treatment, the concentration in drinking water is shown. Statistical significance was determined by Fisher's exact test for comparing control $p53^{172H/H}$ mice to the respective genotype or treatment condition. * $P < 0.05$, ** $P < 0.01$, *** $P < 0.0001$

Supplemental Table 2. Characteristics of LFS patients in metformin study

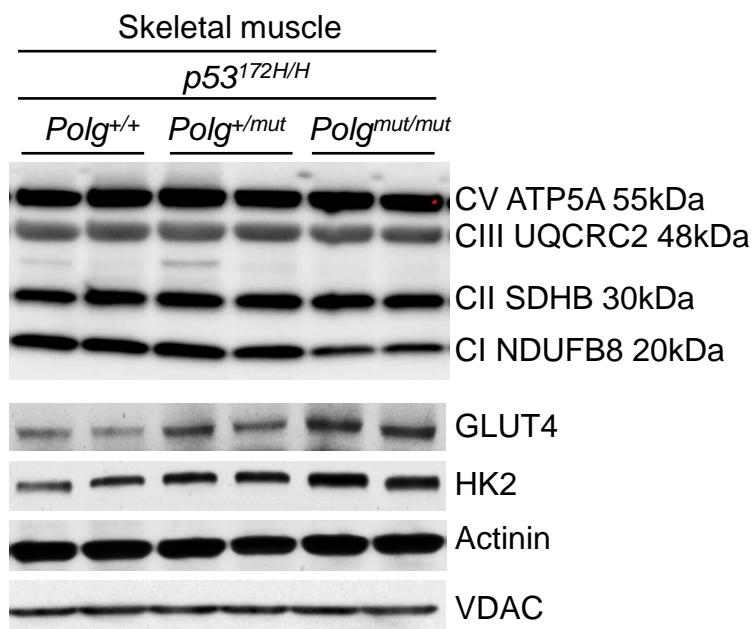
Subject	Age	Gender	p53 amino acid change
1	46	F	R273H
2	48	F	P222L, R267W
3	26	F	122X
4	33	M	R283C
5	19	M	P219S
6	46	F	P219S
7	33	F	Exon1-8del
8	39	F	V122D
9	51	F	L194F
10	38	F	Exon1del
11	41	F	R267Q
12	31	M	P72R
13	41	F	R267N
14	41	F	T125T*
15	44	F	V218G
16	54	M	Exon1-8del
17	39	F	R248Q

*The 12299 G>A (Thr125Thr) alteration in exon 4 of *TP53* has been reported in LFS families and affects the splice donor site, leading to expression of an aberrant mRNA species (9, 10).

References

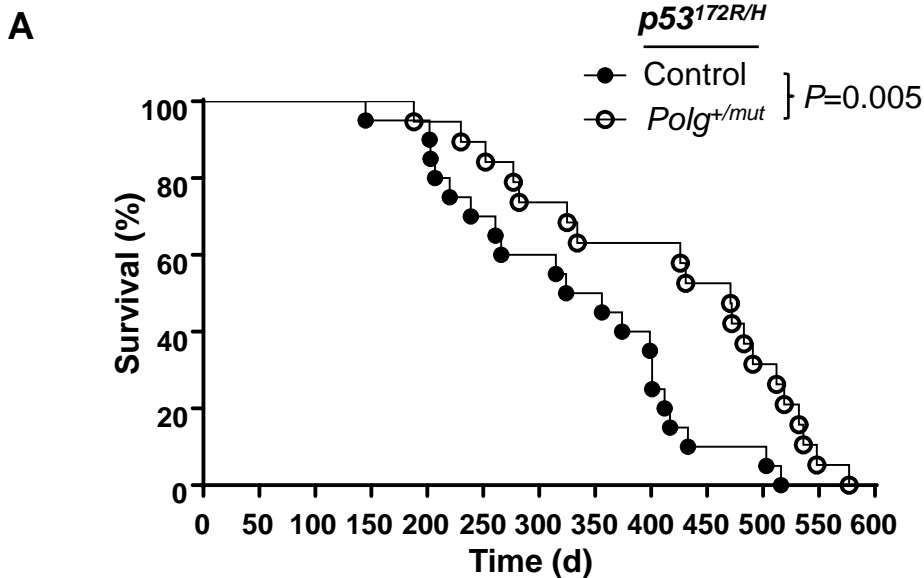
1. Walcott FL, Hwang PM, Wang PY, Savage SA, Mai P, Steinberg SM, Pollak MN, Dennis PA, and Fojo AT. Design of a phase I chemoprevention study of metformin and Li-Fraumeni syndrome (LFS). *Cancer Research*. 2014;74(23).
2. Lang GA, Iwakuma T, Suh YA, Liu G, Rao VA, Parant JM, Valentin-Vega YA, Terzian T, Caldwell LC, Strong LC, et al. Gain of function of a p53 hot spot mutation in a mouse model of Li-Fraumeni syndrome. *Cell*. 2004;119(6):861-72.
3. Kujoth GC, Hiona A, Pugh TD, Someya S, Panzer K, Wohlgemuth SE, Hofer T, Seo AY, Sullivan R, Jobling WA, et al. Mitochondrial DNA mutations, oxidative stress, and apoptosis in mammalian aging. *Science*. 2005;309(5733):481-4.
4. Memmott RM, Mercado JR, Maier CR, Kawabata S, Fox SD, and Dennis PA. Metformin prevents tobacco carcinogen--induced lung tumorigenesis. *Cancer Prev Res (Phila)*. 2010;3(9):1066-76.
5. Matsumoto T, Wang PY, Ma W, Sung HJ, Matoba S, and Hwang PM. Polo-like kinases mediate cell survival in mitochondrial dysfunction. *Proc Natl Acad Sci U S A*. 2009;106(34):14542-6.
6. Wang PY, Ma W, Park JY, Celi FS, Arena R, Choi JW, Ali QA, Tripodi DJ, Zhuang J, Lago CU, et al. Increased oxidative metabolism in the Li-Fraumeni syndrome. *N Engl J Med*. 2013;368(11):1027-32.
7. van der Windt GJ, Everts B, Chang CH, Curtis JD, Freitas TC, Amiel E, Pearce EJ, and Pearce EL. Mitochondrial respiratory capacity is a critical regulator of CD8+ T cell memory development. *Immunity*. 2012;36(1):68-78.
8. Frezza C, Cipolat S, and Scorrano L. Organelle isolation: functional mitochondria from mouse liver, muscle and cultured fibroblasts. *Nat Protoc*. 2007;2(2):287-95.
9. Warneford SG, Witton LJ, Townsend ML, Rowe PB, Reddel RR, Dallapozza L, and Symonds G. Germ-Line Splicing Mutation of the P53-Gene in a Cancer-Prone Family. *Cell Growth & Differentiation*. 1992;3(11):839-46.
10. Varley JM, McGown G, Thorncroft M, Santibanez-Koref MF, Kelsey AM, Tricker KJ, Evans DG, and Birch JM. Germ-line mutations of TP53 in Li-Fraumeni families: an extended study of 39 families. *Cancer Res*. 1997;57(15):3245-52.

Supplemental Figure 1

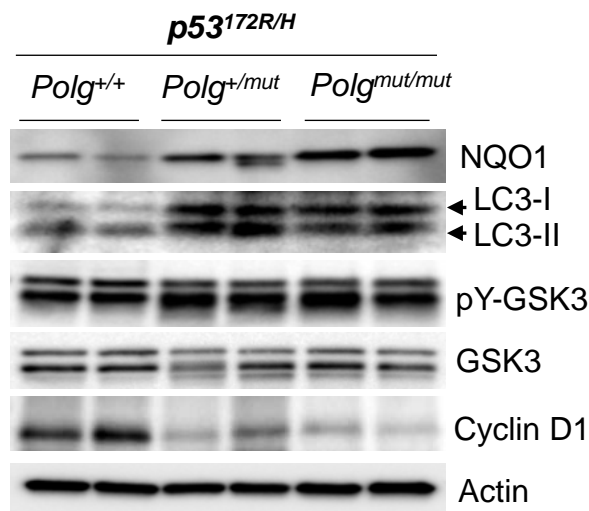


Supplemental Figure 1. *Polg* mutant allele dose-dependent decrease in mitochondrial complex I subunit and increase in glycolytic protein expression in skeletal muscle. Decreased levels of mitochondrial complex I (CI) associates with increased levels of glucose transporter 4 (GLUT4) and mitochondrial hexokinase 2 (HK2) involved in glycolysis in *Polg* mutant skeletal muscle. The gastrocnemius muscles of ~10 wk old mice were processed for immunoblotting. Skeletal muscle actinin and VDAC serve as loading controls for cytosolic and mitochondrial proteins, respectively.

Supplemental Figure 2

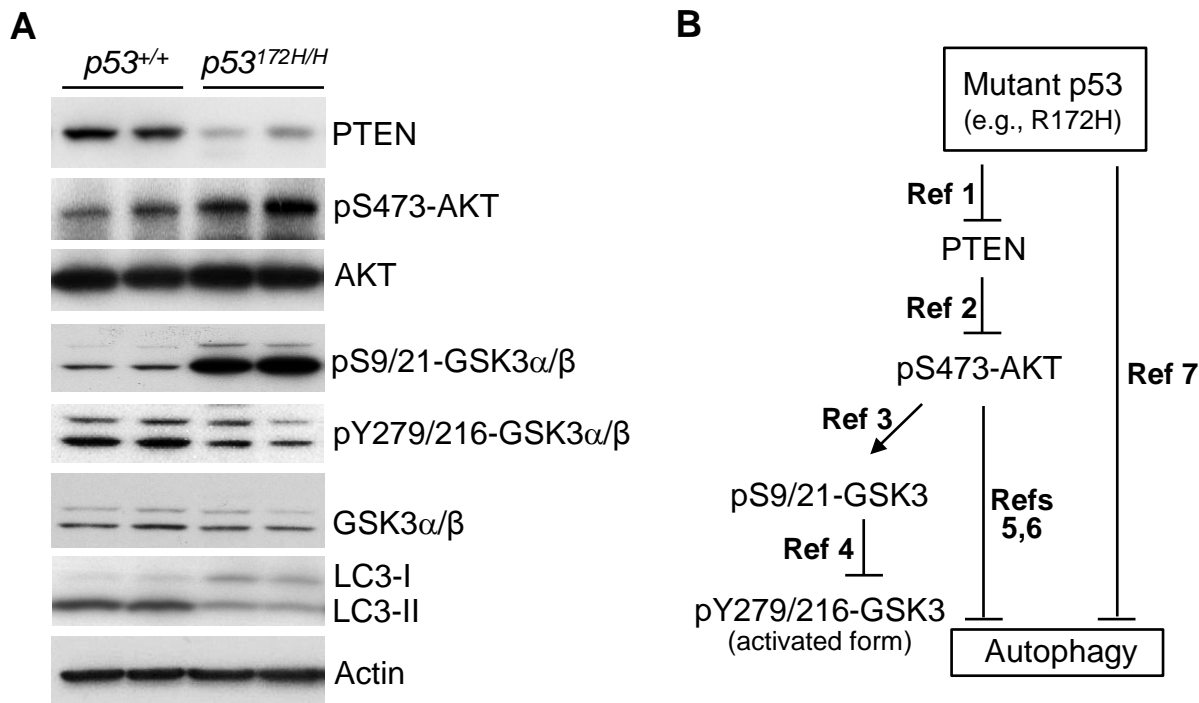


B



Supplemental Figure 2. *Polg* mutation activates the anti-proliferation signaling and increases the survival time of heterozygous *p53^{172R/H}* mice, the genotype that causes LFS in humans. (A) Kaplan-Meier survival plot of *p53^{172R/H}* control (n=20) and *Polg^{+/mut} p53^{172R/H}* double mutant (n=19) female mice. The median survival time of *p53^{172R/H}* mice was increased from 340 d to 471 d by introducing the heterozygous *Polg* mutation. Remarkably, the relative increase of ~40% was similar to that observed in homozygous *p53^{172R/H}* mice (Figure 1B). Statistical differences were detected by the log-rank test. (B) Immunoblots of spleen samples obtained from ~1 yr old *Polg^{+/+}*, *Polg^{+/mut}* and *Polg^{mut/mut}* mice in *p53^{172R/H}* background.

Supplemental Figure 3

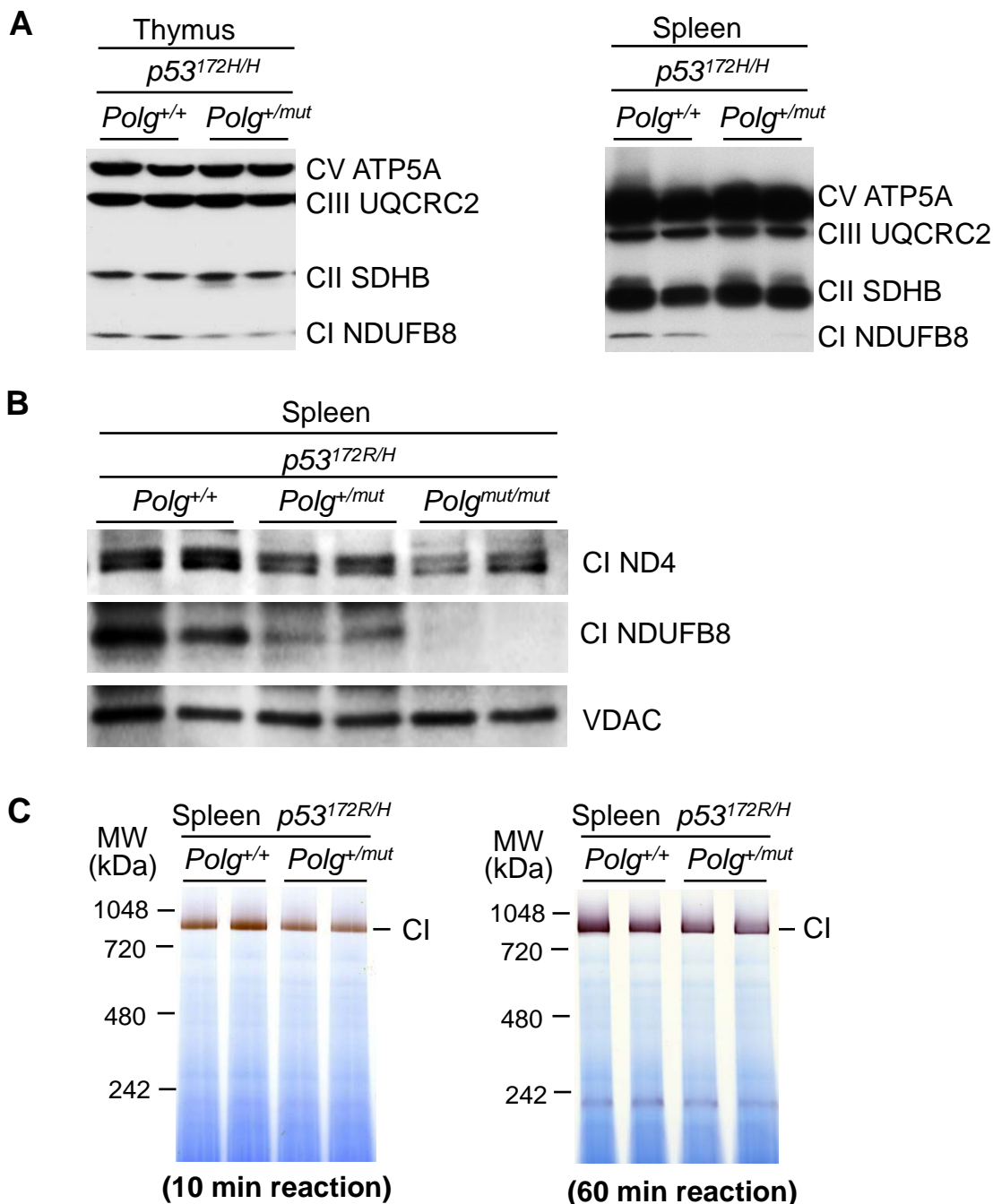


Supplemental Figure 3. Mouse p53 R172H mutant can inhibit GSK3 and autophagy via PTEN-AKT pathway in mice. (A) Immunoblots of thymus tissue of ~10 wk old male mice of the indicated genotypes. (B) Pathway diagram with corresponding references for the mechanisms by which p53 R172H can promote tumorigenesis by inhibiting GSK3 signaling and autophagy.

Supplemental figure 3B references:

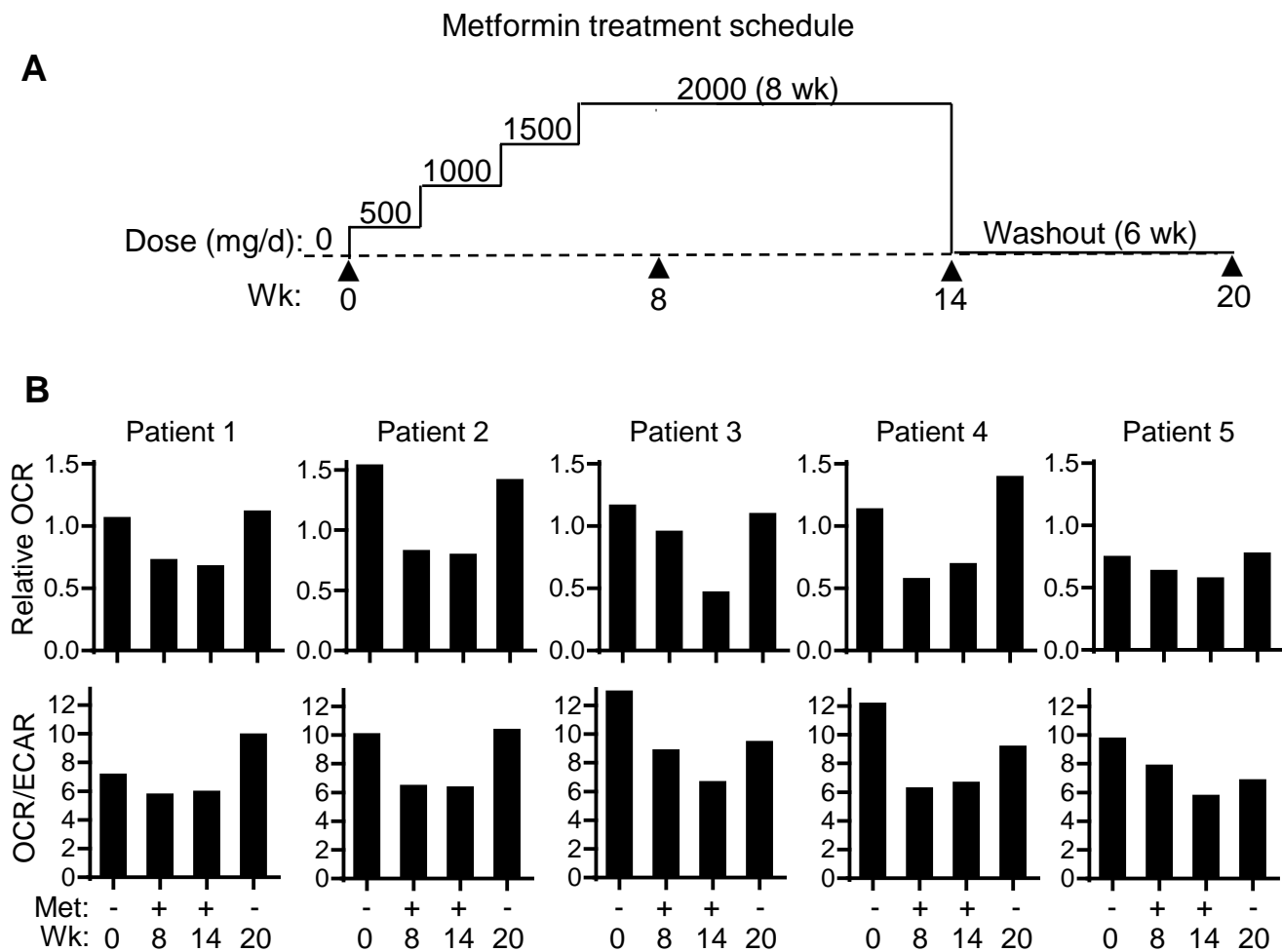
1. Stambolic V, et al. Regulation of PTEN transcription by p53. *Mol Cell*. 2001;8(2):317–325.
2. Cantley LC, et al. New insights into tumor suppression: PTEN suppresses tumor formation by restraining the phosphoinositide 3-kinase/AKT pathway. *Proc Natl Acad Sci USA*. 1999;96(8):4240–4245.
3. Cross D, et al. Inhibition of glycogen-synthase kinase 3 by insulin mediated by protein kinase B. *Nature*. 1995;378:785-789.
4. Dajani R, et al. Crystal structure of glycogen synthase kinase 3 β . *Mol Cell*. 2001;105:721–732.
5. Guo X, et al. AKT-mTOR pathway mediates mutant p53 gain-of-function by inhibiting autophagy. *Cancer Res*. 2012;72(8 Suppl):AACR Abstract nr 1173 (doi:10.1158/1538-7445.AM2012-1173).
6. Wang RC, et al. Akt-mediated regulation of autophagy and tumorigenesis through Beclin 1 phosphorylation. *Science*. 2012;16;338(6109):956-959.
7. Morselli E, et al. Mutant p53 protein localized in the cytoplasm inhibits autophagy. *Cell Cycle*. 2008;7(9)3056-3067.

Supplemental Figure 4



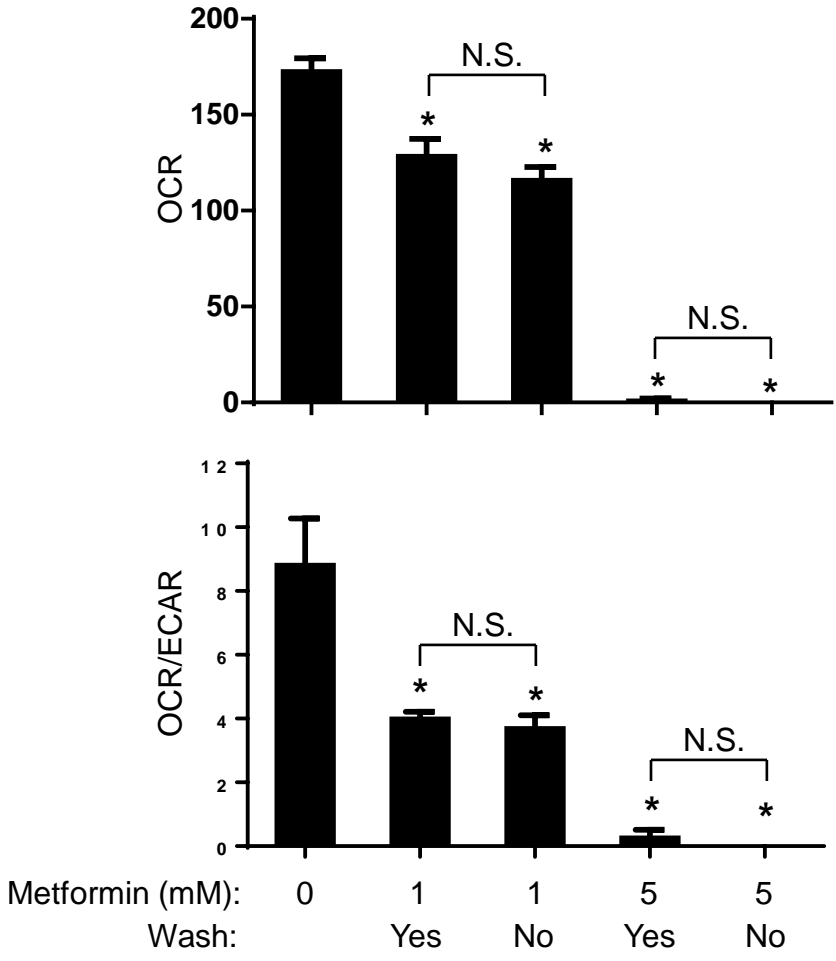
Supplemental Figure 4. *Polg* mutation decreases mitochondrial complex I in LFS mice. (A) Oxphos complex immunoblot of thymus and spleen tissue of *Polg*^{+/+} and *Polg*^{+/*mut*} mice in homozygous *p53*^{172H/H} mutant background (age-matched, 10 and 20 wk old). (B) Further characterization of decreased complex I (CI) subunit levels in spleen of ~1 yr old *Polg*^{+/+}, *Polg*^{+/*mut*} and *Polg*^{*mut/mut*} mice in heterozygous *p53*^{172R/H} background. Note the greater decrease in nuclear-encoded NDUFB8 subunit compared with mtDNA-encoded ND4 subunit. (C) Decreased complex I enzymatic activity in splenic mitochondria of *Polg*^{+/*mut*} compared with *Polg*^{+/+} mice in heterozygous *p53*^{172R/H} background (~1 yr old) as visualized by NBT reaction on blue-native gel at 10 and 60 min time points.

Supplemental Figure 5



Supplemental Figure 5. Representative metabolic assays of mononuclear cells obtained from LFS patients in the metformin treatment clinical protocol. (A) Outline of LFS patient metformin treatment schedule. (B) Blood mononuclear cells were isolated from LFS patients before (week 0), during (week 8 and 14), and after (week 20) metformin (Met) treatment. Relative oxygen consumption rate (OCR) and the ratio of OCR to extracellular acidification rate (ECAR) as an index of oxidative metabolism were measured on Seahorse XF-24 plates. Note recovery pattern of mitochondrial respiration after 6 wk of metformin washout (week 20). Values are the average measurements of at least 5 replicate wells.

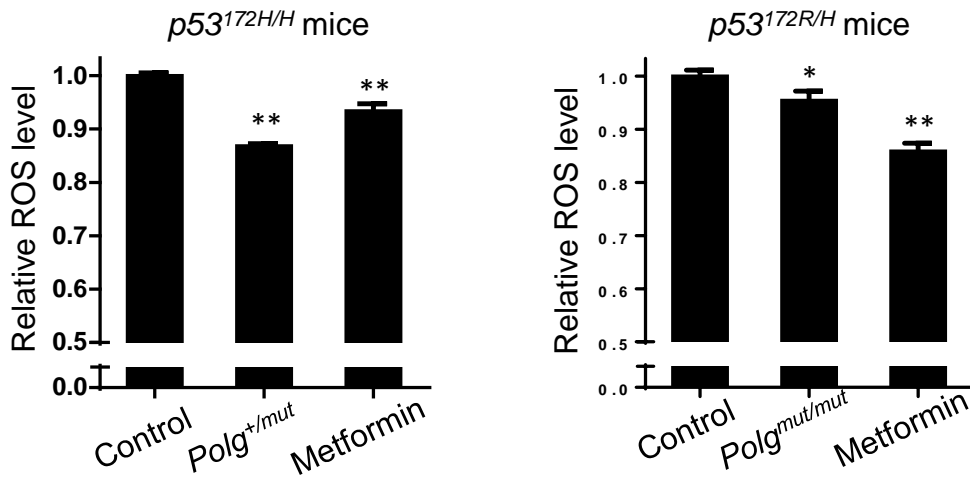
Supplemental Figure 6



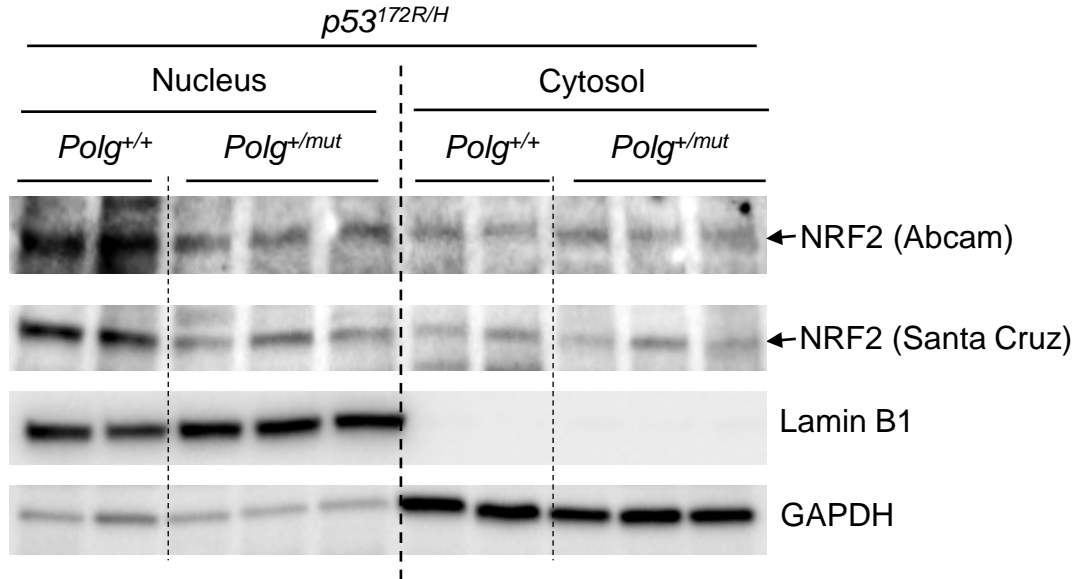
Supplemental Figure 6. Acute removal of metformin prior to the Seahorse assay does not affect metabolic measurements. HCT116 cells were incubated overnight with metformin at the indicated concentrations. After treatment, metformin was either washed away or kept in the medium for the duration of the Seahorse metabolic assay. Oxygen consumption rate (OCR) and extracellular acidification rate (ECAR) were measured (n ≥ 3). Statistical differences were detected by 1-way ANOVA test and 2-tailed *t* test for two sample comparison. N.S. (nonsignificant), **P* < 0.01.

Supplemental Figure 7

A

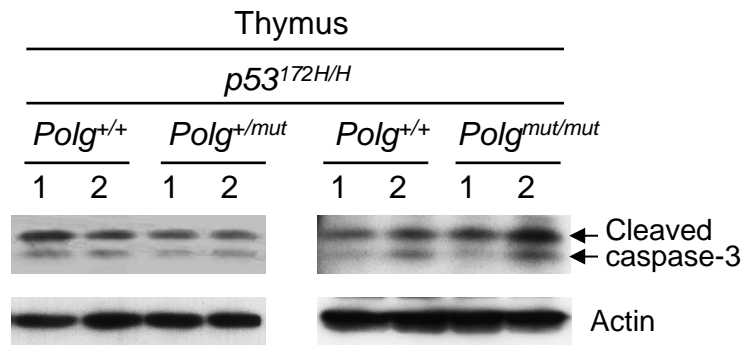


B



Supplemental Figure 7. Markers of oxidative stress are reduced by *Polg* mutation and metformin treatment in LFS mice. (A) ROS levels were measured in thymus cells of male LFS mice (10 wk old) with either *Polg* mutation or 3 wk of metformin treatment (1.25 mg/ml drinking water). Dissociated thymus cells were stained with DCF and quantified by flow cytometry ($n \geq 3$). (B) Nuclear and cytosolic fractions were obtained from spleens of ~1 yr old mice of the indicated genotypes. Subcellular localization of NRF2 was determined by immunoblotting using NRF2 antibody obtained from two independent sources as indicated. Lamin B1 and GAPDH were used as nuclear and cytosolic markers, respectively. Statistical differences were detected by 1-way ANOVA. * $P < 0.05$, ** $P < 0.01$.

Supplemental Figure 8



Supplemental Figure 8. Increased apoptosis is associated with homozygous, but not heterozygous, *Polg* mutation in the LFS mouse model. Immunoblots of thymic tissue obtained from ~10 wk old male mice of the indicated genotypes. Compared with the ~40% relative increase in median survival time of *p53*^{172H/H} mice caused by heterozygous *Polg* mutation, the increased apoptosis (cleaved caspase 3) in thymus tissue associated with *homozygous* *Polg* mutation may contribute to the greater relative increase in survival (~80%) (Figure 1B).